encit 2020

ABCM
Associação Brasileira de Engenharia e Ciências Mecânicas

18th Brazilian Congress of Thermal Sciences and Engineering
November 16-20, 2020 (Online)

# ENC-2020-0505
# MODEL VALIDATION OF A FALLING FILM EVAPORATION PROCESS ON A VERTICAL TUBE USING SUBCOOLED WATER

**M. C. Buss, J. C. Passos**

Universidade Federal de Santa Catarina, LEPTEN-Laboratórios de Engenharia de Processos de Conversão e Tecnologia de Energia, Departamento de Engenharia Mecânica, 88.040-970 – Florianópolis-SC

bussmatheus@gmail.com, julio.passos@ufsc.br

**S. C. Janssen, B. P. M. van Esch**

Eindhoven University of Technology, Power and Flow Group, Department of Mechanical Engineering, Gemini-Zuid, Groene Loper, 15, 5612AZ, Eindhoven, The Netherlands.

s.c.janssen@student.tue.nl, B.P.M.v.Esch@tue.nl

***Abstract.*** *Falling Film Evaporators (FFE) are used by a wide range of industrial sectors because of their high heat transfer rate per unit of surface area while maintaining a relatively low temperature difference between surface and liquid. This allows more compact system designs and thereby reduces material costs. Although they have been used for decades the design of these evaporators is still mostly based on estimates and empirical data. The available literature is reviewed as foundation for the mathematical model made for a vertical FFE design using subcooled water. Dimensionless numbers are used to fundamentally compare its results with literature. Additionally, simulations are performed to validate the model. An experimental setup of a vertical FFE was built in LEPTEN, at UFSC. An overview of its construction and improvements is provided. This setup is used as a basis for the model, which means it can be used to validate the theory in future works.*

***Keywords:*** *Vertical Falling Film Evaporator, heat and mass transfer, Modelica modeling, subcooled water, evaporation*

## 1. INTRODUCTION

Falling Film Evaporators (FFE) are used by a wide range of industrial sectors because of their high heat transfer rate per unit of surface area while maintaining a relatively low temperature difference between surface and liquid. This allows more compact system designs and thereby reduces material costs. FFE are used by the food sector (dairy products or fruit juices for example) (Gourdon *et al.* (2015)), for water desalination, nuclear engineering (Huang *et al.* (2015)) among others. Although they have been used for decades the design of these evaporators is still mostly based on estimates and empirical data. Therefore, mathematical models should be created and validated to be able to better design a FFE. With the aim of providing these models within an open source code this research uses Modelica as a programming language.

Modelica (Modelica Association (2007)) shows to be suitable software for modelling thermal systems because of its component-based equation solver and its ability to implement physical equations independent from their numerical solutions (Assaf *et al.* (2011)). de la Calle *et al.* (2012) successfully implemented a full horizontal FFE in Modelica with submodels to describe the physical behaviour of each component. However, there is no implementation of a vertical FFE model in Modelica yet. Since some industrial sectors use the evaporator in a vertical orientation it is important to develop this mathematical model as well. This research aims to create this model and compare it with experimental results.

To obtain these results an experimental setup of a vertical FFE was built in the Laboratory of Energy Conversion Engineering and Energy Technology, LEPTEN, at the Federal University of Santa Catarina, UFSC. An overview of its construction and improvements is presented, following the works of de Souza (2018) and Jansen (2019) on aspects such as the inflow distribution and direction, thermocouple placement for temperature measurements and modifications to increase the surface area using grooves. Additionally the authors describe their work on the setup regarding improved visualisation for future measurements.

Due to the Covid-19 outbreak, LEPTEN was closed so no experimental results could be obtained. The film thickness is predicted with a simulation model. It is compared with experimental data of other authors and available theory.

## 2. THEORY

The **heat flow rate** ($q$) for convection as described by equation 1 is a measure that helps to describe the performance of a FFE by indicating the amount of heat exchange done by the FFE. It takes into account the heat transfer coefficient ($h$), surface area ($A$), and the difference between the wall temperature ($T_w$) and film temperature ($T_f$).

$$q = hA\Delta T = hA(T_w - T_f) \tag{1}$$

In order to improve the performance, the heat flow rate should be increased as much as possible. There is a limit in increasing $\Delta T$ because of temperature restrictions for the fluids used (milk, juice etc.). This work will mainly focus on the evaluation of the convective heat transfer coefficient for a fixed area and a fixed heat flow by the heating element. The variable h is dependent of the mass flow rate and thereby of the Reynolds number.

The **Reynolds number** is a dimensionless parameter used for evaluating the flow regime, usually having transition values between the regimes (e.g. laminar to turbulent). Effectively it expresses the ratio between inertial and viscous forces. It considers the mass flow rate ($\dot{m}$), dynamic viscosity($\mu$) and tube diameter ($D$). For a cylindrical thin film the Reynolds number is defined as shown in equation 2. The film thickness defines the characteristic length and is included within the mass flow rate.

$$Re = \frac{4\Gamma}{\mu} = \frac{4\dot{m}}{\mu\pi D} \tag{2}$$

Transition values for Reynolds are widely available in literature, but mutual agreement between sources is rare. Some authors provide discrete values, others calculate it based on dimensionless parameters, those being either Prandtl or Kapitza. Some authors consider only the laminar and turbulent flow regimes, some take into account a wavy regime between the two. It is also common to define a transition region between regimes. Several empirically obtained regime transitions found in literature are listed in table 1.

Table 1: Reynolds transition values for a thin film according to literature.

**Based on Prandtl number**

| Authors | Value | Flow regime |
|---|---|---|
| *Chun and Seban (1971)* | $5800/Pr^{1.06} = 1810$ | Turbulent |
| *Wilke (1962)* apud Aviles (2007) | $2460/Pr^{0.65} = 1204$ | Turbulent |

**Discrete value**

| Authors | Value | Flow regime |
|---|---|---|
| *Ticona (2003) apud Teleken (2013)* | 25 | Wavy |
| | 1000 | Turbulent |
| *Nusselt (1916) apud Teleken (2013)* | 1600 | Turbulent |
| *Baehr and Stephan (2006)*[AB] | 47 | Wavy |
| | 611 | Transition 2 |
| | 1600 | Turbulent |

**Based on Kapitza number**

| Authors | Value | Flow regime |
|---|---|---|
| *Ishigai* et al. *(1972)*[B] | 56 | Transition 1 |
| | 263 | Wavy |
| | 300 | Transition 2 |
| | 1600 | Turbulent |
| *Al-Sibai (2004)*[B] | 36 | Transition 1 |
| | 60 | Wavy |
| | 1150 | Transition 2 |
| | 3915 | Turbulent |

[A] Authors are using condensing films
[B] Authors define Reynolds as $Re = \dot{m}/(\mu b)$ so the values have been multiplied by 4

The **Prandtl number** describes the ratio of momentum diffusivity over heat diffusivity and consists only of fluid properties that are either temperature or pressure dependent (dynamic viscosity, specific heat capacity ($c_p$) and thermal conductivity ($k$)). Equation 3 shows that relation.

$$Pr = \frac{\nu}{\alpha} = \frac{(\mu/\rho)}{(k/\rho c_p)} = \frac{\mu c_p}{k} \tag{3}$$

Additionally, the **Kapitza number** expresses the ratio between the surface tension forces and viscous forces on the

waves along the falling film. The Kapitza number is a function of fluid properties (surface tension ($\sigma$), density ($\rho$) and kinematic viscosity ($\nu$)) and gravity's acceleration. The dimensionless number is thereby interesting to evaluate the film uniformity for different fluids. Equation 4 is used to calculate it.

$$Ka = \frac{\sigma}{\rho g^{1/3} \nu^{4/3}} \tag{4}$$

The **film thickness** ($\delta$) and the convective heat transfer coefficient are inversely proportional according to the Nusselt number (equation 7), which means that an increase in the film's thickness causes a decrease in the heat transfer coefficient and vice versa. So it's desirable that the film remains as thin as possible. However when the film is too thin any perturbation can severely compromise the film's integrity and uniformity and thereby originate undesirable dry patches. Therefore it is important to correctly model the film thickness.

In practice most falling films are outside the laminar regime, having waves and turbulence effects on the film. Beyond that, even on laminar films thickness measurements are difficult to make. Therefore several empirical correlations are available in literature to estimate the thickness. These correlations can be generalized by equation 5. The coefficients $c_i$ have different values for each author as shown in table 2. Equation 5 shows that the film thickness tends to increase as $Re$ increases, as long as $c_3$ is positive.

$$\delta = c_1 \left( \frac{v^2}{g} \right)^{c_2} \mathrm{Re}^{c_3} \qquad \text{Reynolds range: } c_4 \tag{5}$$

Table 2: Coefficient values for film thickness calculation.

| **Authors** | $c_1$ | $c_2$ | $c_3$ | $c_4$ |
|---|---|---|---|---|
| *Stephan* et al. *(2010)*[A] | 1.4422[B] | 1/3 | 1/3 | Re<400 |
| | 0.4356 | 1/3 | 8/15 | Re>400 |
| *Nusselt (1916), Chun and Seban (1971), Teleken (2013)* | 0.9086 | 1/3 | 1/3 | Re<1600 |
| | 0.2628 | 1/3 | 1/3 | Re>1600 |

[A] Equation for turbulent regime is empirically obtained and agrees well with correlations from 4 papers cited in this source.
[B] Allowance for surface waves in the laminar regime can be made by changing this value to 2.4 according to Kapitza (1948, 1949).

In figure 1, the thickness equations are compared with experimental results by Zhang *et al.* (2000), who used an optical-electronic method to measure the film thickness on a vertical tube falling film.

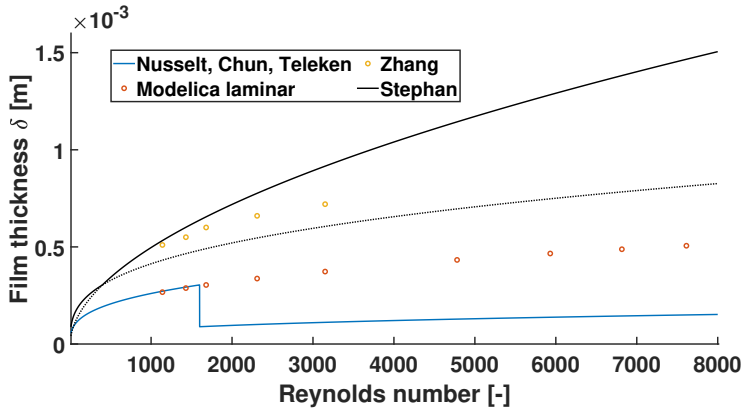


Figure 1: Film thickness $\delta$ for different Reynolds numbers. Results by Zhang *et al.* (2000) are close to Stephan *et al.* (2010). There is a discontinuity in the equations by Nusselt (1916), Chun and Seban (1971) and Teleken (2013). The Modelica model is based on their laminar equation for the full Reynolds range.

Figure 1 shows a major difference between the two pieces of literature. In order to verify a suitable relation for the thickness over the Reynolds number, additional experiments should be performed and fitted to a curve. That fit can be used for the final Modelica model.

**Weber's number** expresses the ratio between inertial forces over surface tension. If the falling velocity gets too high, the inertial forces become dominant resulting in an unstable film. Therefore the Weber number dictates a maximum flow rate for a stable film based on the fluid properties and the film thickness. It is defined in equation 6.

$$We = \frac{\rho \nu^2 \delta}{\sigma} \tag{6}$$

When experimental results yield an appropriate relation (curve fit) for $\delta$, the Weber number can be calculated over the Reynolds domain. By comparing the uniformity during experiments and the related Weber numbers, a critical Weber number can be obtained. It can be used in Modelica to find flow rate restrictions.

The **Nusselt number** is a dimensionless parameter describing the ratio between the convective and conductive heat transfer in a fluid. The Nusselt number is stated in equation 7.

$$Nu = \frac{h\delta}{k} \implies h = \frac{Nuk}{\delta} \tag{7}$$

Many empirical correlations have been proposed to allow the determination of the Nusselt number with only the knowledge of $Re$ and $Pr$ as denoted by equation 8. These correlations are determined by the value of empirically obtained constants ($c_1$, $c_2$ and $c_3$) and are valid for a certain condition (A flow regime or Reynolds number).

$$Nu = c_1 Re^{c_2} Pr^{c_3} \quad \text{for} \quad Condition \tag{8}$$

The simulations allow to calculate the values for the thickness and the heat transfer coefficient independently from the Nusselts number. That means that the final results don't rely on empirically obtained data. Among the literature several constants have been proposed. Table 3 shows some of the correlations that were used to compare the data. It contains the constants and the conditions to be valid, as defined by the authors.

Table 3: Coefficient values and their conditions to be valid for Nusselt calculation

| **Authors** | $c_1$ | $c_2$ | $c_3$ | Condition |
|---|---|---|---|---|
| Stephan *et al.* (2010) | 1.43 | −0.33 | 0 | Laminar[A] |
| | 0.0425 | 0.2 | 0.344 | Transition[A] |
| | 0.0136 | 0.4 | 0.344 | Turbulent flow[A] |
| Chun and Seban (1971) | 0.82 | −0.22 | 0 | Re < 1890 |
| | 0.0038 | 0.4 | 0.65 | Re > 1890 |
| Baehr and Stephan (2006) | 0.069 | −0.33 | 0 | Re < 155 |
| | 0.0325 | 0.25 | 0.5 | Re > 155 |

[A] The authors state that the highest Nu value per Reynolds number of the three equations should be used.

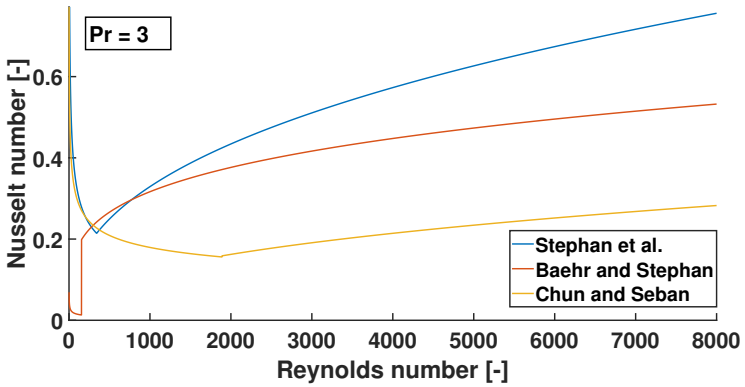


Figure 2: Nusselt number for different Reynolds numbers according to Stephan *et al.* (2010), Baehr and Stephan (2006) and Chun and Seban (1971) for water at 60°C and ambient pressure. The Nusselt number from Baehr and Stephan (2006) shows a sudden jump at its Reynolds transition number, while the one from Stephan *et al.* (2010) shows a sharp transition point.

The **convective heat transfer coefficient** measures the effectiveness of the heat exchanger. By rewriting equation 1 equation 9 can be obtained.

$$h = \frac{q}{A\Delta T}; \quad \Delta T = T_w - T_f; \implies h = \frac{q}{A(T_w - T_f)} \tag{9}$$

Also from inserting data from equations 5 and 8 into equation 7 it is possible to calculate $h$ without having the temperature data. With that figure 3 can be obtained from the available authors.

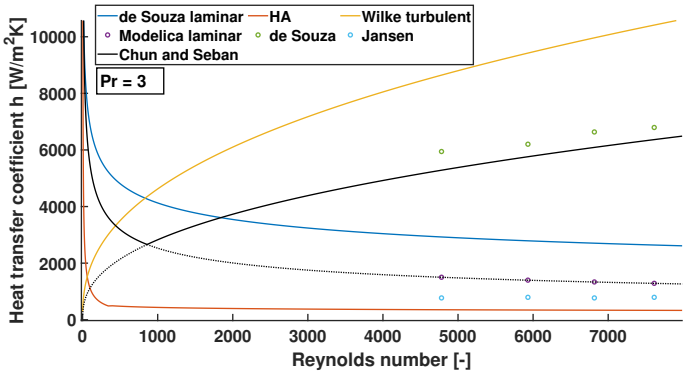


Figure 3: Heat transfer coefficient for different Reynolds numbers. All equations are plotted over the full domain to show that the laminar equations of Chun and Seban (1971) are implemented on the Modelica model over the full Reynolds range. de Souza (2018) uses the same equation for the turbulent regime as Chun and Seban (1971). Experimental results from de Souza (2018) are close to the turbulent equation of Chun and Seban (1971), The results from Jansen (2019) are closer to the theory of the Heat Atlas (HA) by Stephan *et al.* (2010). In experiments, Jansen (2019) used a grooved surface instead of the smooth surface by de Souza (2018).

## 3. EXPERIMENTAL

In order to validate the simulations, experimental data are required. This data are obtained using the experimental setup of a vertical FFE assembled in LEPTEN at the Mechanical Engineering Department of UFSC. The setup is shown schematically in figure 4a.

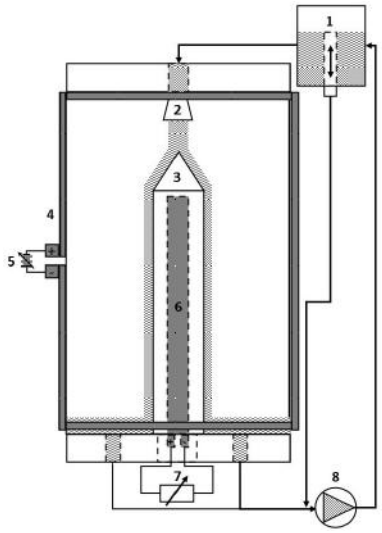


(a) Schematic of the setup used: 1) Flowrate regulator by adjustable tube, 2) Sponge disk and wire mesh to uniformly spread the water, 3) Teflon cone to distribute the water over the stainless steel cylinder evenly. 4) Resistance wire used to heat the glass tube to prevent condensation and thereby improve visualisation, 5) Variable DC power supply, 6) Electrical cartridge resistance for heating the FFE, 7) Power supply: JNG I1215426, 8) Thermal bath and pump.

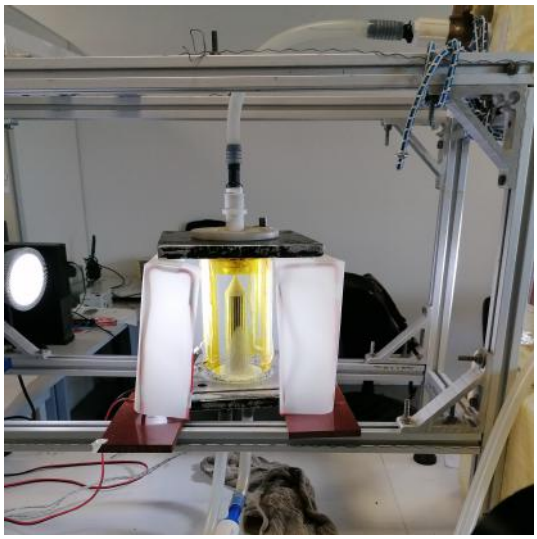

(b) Picture of most of the setup. In addition to figure 4a lamps and a paper cover are added to fully diffusely light the FFE and thereby improve visualisation of the film.

Figure 4: Experimental setup in LEPTEN

The outer metallic cylinder (D = 31.75mm, L=116mm) surface of the FFE itself has small laser machined grooves, which increase the surface area by $3\%$ when compared to a smooth tube. The grooves were an attempt by Jansen (2019) to increase the wet contact area and thereby increase the amount of heat transfer according to equation 1. Additionally he investigated varying the inflow angle using a funnel. That resulted in an improved distribution due to the tangential flow but also caused splashes and the prototype was less reliable. The combination of a sponge disk and a wire mesh (as mentioned in the caption of figure 4a) still provided the best result for the inflow.

Water is preheated to 60°C using a MQBMP-01 thermal bath from the company MicroQuimica Ltda.. The thermal bath has a pump that is used for circulation through the system. The fluid is not saturated so there is no boiling (evaporation only), preventing bubble generation that could cause hydrodynamic instability, interfering with the film's uniformity. An unstable film could lead to the formation of unwetted areas (dry patches) that reduce the heat transfer area with the film. The mass flow rate is varied to evaluate heat transfer for different Reynolds numbers.

In order to collect temperature data, thermocouples attachment methods to the FFE have been evaluated. The method to be adopted should take into account the fragile nature of the film's uniformity and distort the measurements as little as possible. de Souza (2018) tried using threadlocker adhesive to fix the thermocouples, but had some difficulties and opted to use rivets instead. Jansen (2019) also looked into attachment methods and tried using epoxy glue, welding and soldering, all of them without much success. His final solution was to use thermal tape, acknowledging that it was not an optimal method and suggested that welding may be a viable alternative.
The use of a sealing silicon glue was tested and discarded due to a bad connection with the wall. The main options considered were welding a thicker thermocouple and cyanoacrylate glue.

The entire cylinder is surrounded by a glass tube to reduce ambient interference. To prevent condensation and enable visualisation, the tube is heated using a resistance wire. The wire is fixed with heat resistant tape in a way that does not interfere with front side visualization.

According to Zhang *et al.* (2000) the measurement of the falling liquid film thickness is of critical importance but complicated to be accurately obtained. Studies have been done to measure the thickness with probes that touch liquid's surface. This approach has been used by Härkonen (1994), whilst acknowledging that the method is invasive and could lead to interference with the quantity to be measured. Therefore Zhang *et al.* (2000) devised a method using lasers to measure the thickness without interfering with the film's flow. Aviles (2007) stated a table with an overview of multiple intrusive and non-intrusive methods. For this experimental setup, it is intended to use an optical method in the future to visualise and measure the film thickness.

## 4. Modeling

Within Modelica there are several native libraries available. Three of them were mainly used. Modelica.Fluid was used to implement a fluid flow into and out of the model, as well as setting the ambient temperature and pressure. Modelica.Media was incorporated to model the working fluid and make it possible to switch to other fluids. Modelica.Thermal was the last one to be implemented, it provides the heat source for the system. Those three libraries work with the FFE block created for this work.

The models' assumptions are laminar flow, no shear stress on the liquid-vapour interface, axisymmetric flow, negligible heat transference from the surrounding vapour to the film and conduction is the main heat transfer phenomena, whilst advection is negligible because the film is so thin. Also, due to complexity, wavy effects are not considered. The hydrodynamic equations from Nusselt (1916) model on the film thickness are used because they are based on the same assumptions as mentioned above. The only modification is that the film isn't at saturation temperature, therefore the film's temperature is not constant, but increases over the vertical distance traveled. Because of this complication a numerical approach to solve the equations is chosen. For any given height, the temperature is averaged over the radial distance spanning the film, making the temperature a function of the height of the cylinder only.

The setup is assumed axisymmetric and thereby modeled 2D considering a vertical and radial direction. Using the 2D Navier-Stokes equation in the vertical direction (equation 10) and applying the assumptions above, equation 11 is obtained. Applying the boundary conditions returns the velocity profile in the y direction, as shown in equation 12.

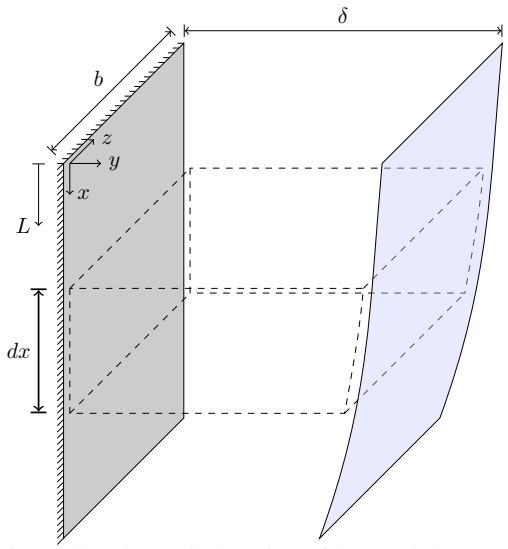


Figure 5: Schematic drawing of the models' control volume (dashed lines), assuming the film is thin enough in comparison to the tube diameter to be flattened

$$\rho\left(\frac{\partial u}{\partial t}+u\frac{\partial u}{\partial x}+v\frac{\partial u}{\partial y}\right)=-\frac{\partial p}{\partial x}+\mu_l\left(\frac{\partial^2 u}{\partial x^2}+\frac{\partial^2 u}{\partial y^2}\right)+\rho_l g \tag{10}$$

$$u=\frac{1}{\mu_l}\left(\frac{\partial p}{\partial x}-\rho_l g\right)\frac{y^2}{2}+c_1 y+c_2$$

$$\begin{cases} @\ y=0: u=0 \Rightarrow c_2=0 \\ @\ y=\delta: \frac{\partial u}{\partial y}=0 \end{cases} \quad \text{and} \quad \frac{\partial p}{\partial x}=\rho_v g \tag{11}$$

$$u_{(y)}=\frac{g}{\mu_l}\left(\rho_l-\rho_v\right)\left(\delta y-\frac{y^2}{2}\right) \tag{12}$$

$$\dot{m}=\int_A \rho_l u dA=\rho_l b\int_0^\delta u dy \implies \dot{m}=\frac{\rho_l b g}{3\mu_l}\left(\rho_l-\rho_v\right)\delta^3 \tag{13}$$

The mass flow rate can be obtained by using equation 12 on the upper surface of the control volume shown in figure 5. The result, equation 13, is the same as the one obtained by Nusselt and is one of the equations used on the Modelica model. An equation for the turbulent regime was not obtained and the attempts to implement a finite elements on Modelica were not successful. Figure 6 shows the energy balance on a slice of the control volume. Equation 14 is the energy balance used by the Modelica model.

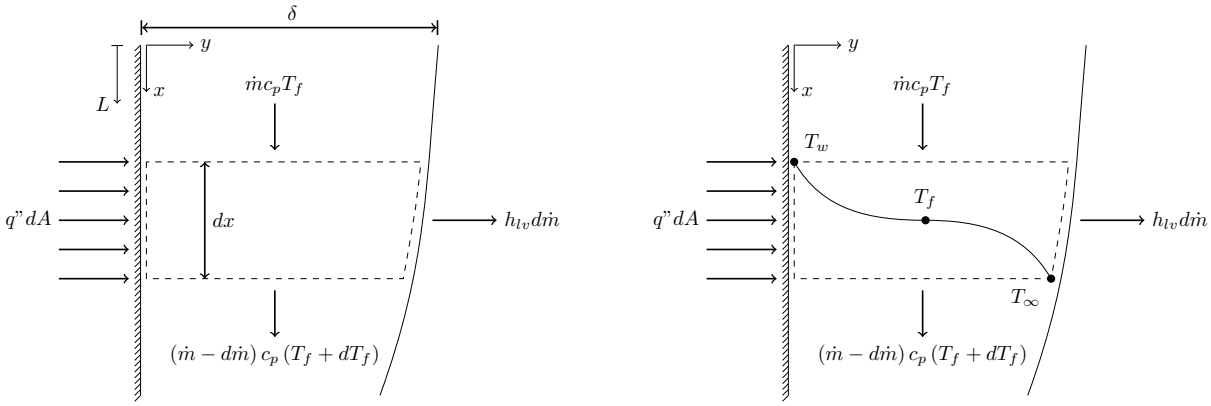


(a) Spatial coordinates for the energy balance.

(b) Temperature profile on the control volume.

Figure 6: Energy balance drawings

$$\dot{m}c_p T_f+q"dA=\left(\dot{m}+d\dot{m}\right)c_p\left(T_f+dT_f\right)+h_{lv}d\dot{m} \tag{14}$$

The last main equation used by the model is equation 1. Having those three equations (1, 13 and 14) and the proper parameters the model is set to solve for thickness, evaporation rate and film temperature. The parameters used are the tube perimeter ($b$), length ($L$), Reynolds number or mass flow rate, ambient pressure and temperature, fluid entrance temperature, heat flow rate and working fluid. Using the equations mentioned and these input parameters, Modelica calculates and provides the required output variables.

Data on horizontal FFEs was found in literature. For comparison, the Modelica model was adjusted. The definition of the Reynolds number was changed to half of equation 2, the length of the tube in the model was considered half the circumference of the horizontal tube and the total area was multiplied by two (two tube halves). Value $b$ is the length of the horizontal tube.

## 5. RESULTS

This section first shows the behaviour of the modeled FFE over its length in figure 7. Additionally the model outcomes are compared to data available in literature.

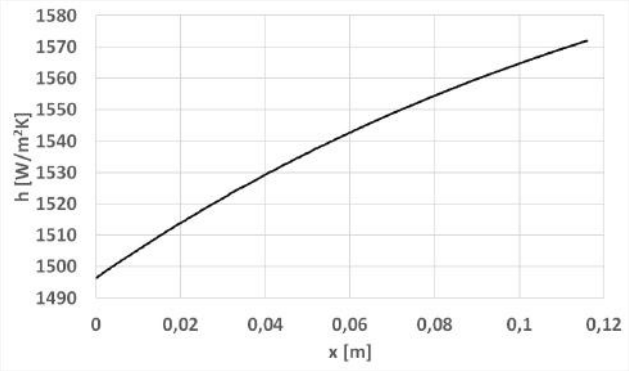


(a) Heat transfer coefficient along the x axis, showing an increase as predicted by equation 9, considering constant heat flow and the increase in temperature shown in figure 7b.

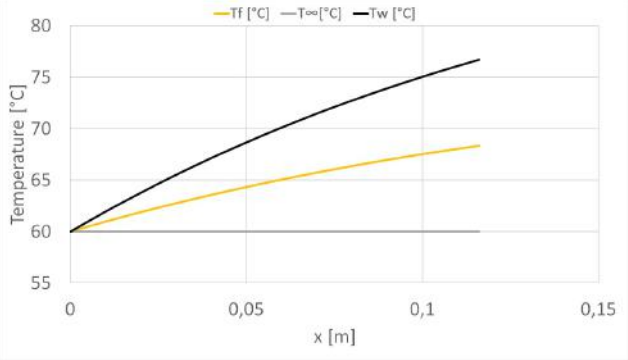


(b) Temperatures along the x axis. The ambient temperature $T_\infty$ is constant, matching the boundary condition. The temperature difference between wall and fluid is positive, resulting in heating of the fluid. Due to the constant ambient temperature and the increased fluid temperature, evaporation takes place (increasing over the length).

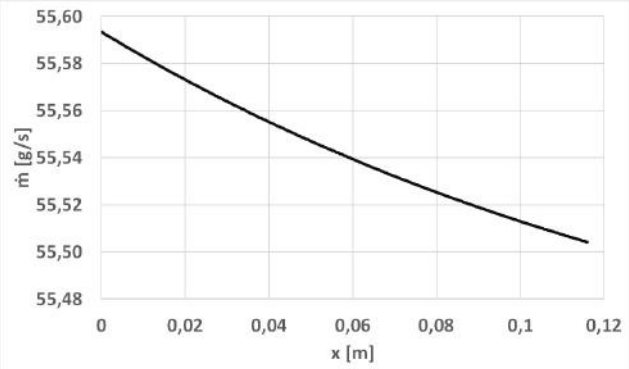


(c) Mass flow rate (liquid) along the x axis is decreasing due to the evaporated liquid.

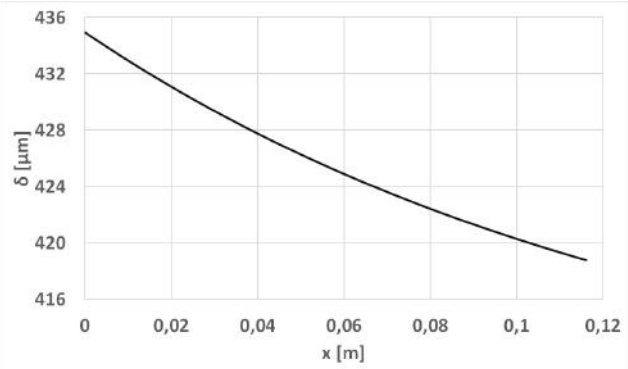


(d) Film thickness along the x axis is decreasing due to evaporation.

Figure 7: Results from the simulations in Modelica. The parameters are those of the LEPTEN experimental setup and Re is set to $4780$ at the fluid's entrance. Additionally the heat supply was set to 284.6 $W$.

Figure 7 shows the expected behaviour from a FFE suggesting the model is functioning in an appropriate manner. The absolute values should now be compared to literature and experiments for complete validation.

Narváez-Romo and Simões-Moreira (2017) obtained experimental data on a horizontal tube FFE which is compared to a horizontal version of our FFE model in figure 8.

It is noted that the Modelica model has a higher slope of temperature along the traveled distance, even though the average remains close on both data sets. This could be due to the increased influence of gravity in the vertical tube as opposed to the horizontal one. The average could make it so the effect of the curvature evens out along the upper and lower halves. From the comparison in figure 8 it is interesting to note that the Modelica model always returns a higher value than the ones computed by the authors.

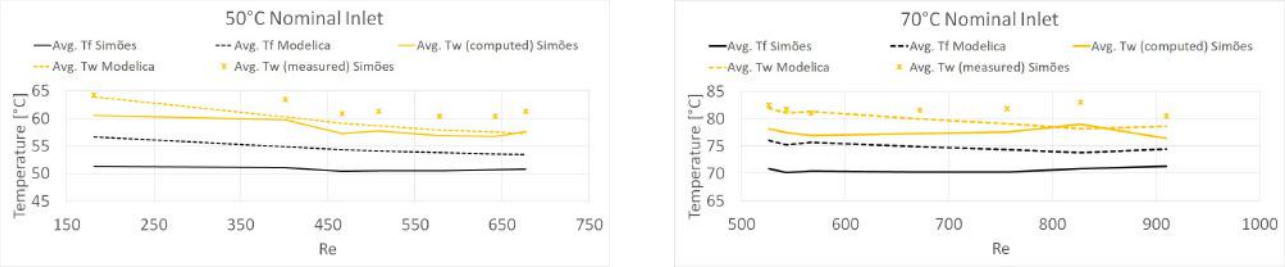


Figure 8: Comparison between average temperatures on the simulated model and experimental data on a horizontal tube for different Reynolds numbers. Experimental data was available for both 50 and 70 degrees Celsius. Thereby there were two simulations performed in Modelica using these inflow temperatures.

## 6. DISCUSSION

There is an experimental difference between the works of Jansen (2019) and de Souza (2018), noted both on the setup and acquired data. Whilst de Souza used a smooth vertical tube Jansen made several longitudinal grooves on the tube in an attempt to increase surface area and thereby increase the heat transfer. The effective area increase was 3% at most, showing little significance. Therefore the grooves were not considered on the final model. The large difference between experimental results obtained by both authors on similar setups is mostly unexplained. Another interest on the grooved surfaces was to increase film stability and prevent dry patches. Unfortunately the model does not take into account film stability and experimental data couldn't be obtained, therefore it was not feasible to evaluate this possible effect.

From figure 3 it can be observed that the model behaves like the laminar one from Chun and Seban (1971) on the full regime despite the water is not at saturation temperature. The correct correlation for the turbulent regime should be empirically determined. Unfortunately due to the Covid-19 pandemic these experiments were interrupted.

For future works it is recommended to:

- Finish setting up the high speed camera at LEPTEN for measurements on film thickness and stability;
- Attach thermocouples to the tube so that the model can be evaluated for its accuracy;
- Develop an approach with less assumptions to solve the problem, so that the turbulent regime can be better represented;
- Evaluate the impact of the grooves on film stability.

## 7. ACKNOWLEDGEMENTS

Thanks to professor Simões-Moreira and PhD student Narváez-Romo from Poli-USP for their availability and cooperation. Thanks to CNPQ and PIBIC for their support to the scientific community.

## 8. REFERENCES

Al-Sibai, F., 2004. *Experimentelle Untersuchung der Strömungscharakteristik und des Wärmeübergangs bei welligen Rieselfilmen.* Ph.D. thesis, RWTH, Aachen, Germany.

Assaf, K., Zoughaib, A. and Clodic, D., 2011. "Modelica-based modelling and simulation of dry-expansion shell-and-tube evaporators working with alternative refrigerant mixtures". In *International Journal of Refrigeration*. Elsevier, Vol. 34, pp. 1471–1482. ISSN 01407007. doi:10.1016/j.ijrefrig.2011.03.010.

Aviles, M.L., 2007. *Experiments on falling film evaporation of a water-ethylene glycol mixture on a surface with longitudinal grooves*. Ph.D. thesis, Technischen Universitat Berlin, Berlin, Germany.

Baehr, H.D. and Stephan, K., 2006. *Wärme- und Stoffübertragung.* Springer-Verlag, Berlin, 5th edition.

Chun, K.R. and Seban, R.A., 1971. "Heat transfer to evaporating liquid films". *Journal of Heat Transfer*, Vol. 93, pp. 391 – 396.

de la Calle, A., Yebra, L.J. and Dormido, S., 2012. "Modeling of a falling film evaporator". In *Proceedings of the 9th International Modelica Conference*. Munich, Germany.

de Souza, J.N., 2018. *Análise experimental do processo de evaporação em película descendente sobre tubo vertical*. Master's thesis, Universidade Federal de Santa Catarina, Florianopolis, Brasil.

Gourdon, M., Innings, F., Jongsma, A. and Vamling, L., 2015. "Qualitative investigation of the flow behaviour during falling film evaporation of a dairy product". *Experimental Thermal and Fluid Science*, Vol. 60, pp. 9 – 19. doi: https://doi.org/10.1016/j.expthermflusci.2014.07.017.

Huang, X.G., Yang, Y.H. and Hu, P., 2015. "Experimental study of falling film evaporation in large scale rectangular channel". *Annals of Nuclear Energy*, Vol. 76, pp. 237 – 242. doi:https://doi.org/10.1016/j.anucene.2014.09.053.

Härkonen, M., 1994. "Heat transfer to evaporating falling films of water and sugar/water solution". *Wärme- und Stoffübertragung*, Vol. 29, pp. 349 – 355.

Ishigai, S., Nakanisi, S., Koizumi, T. and Oyabi, Z., 1972. "Hydrodinamics and heat transfer of vertical falling liquid films". *Bull JSME*, Vol. 15, pp. 594–602. doi:https://doi.org/10.1299/jsme1958.15.594.

Jansen, T.D., 2019. *Water Falling Film Evaporation on a Vertical Tube*. Master's thesis, Eindhoven University of Technology, Eindhoven, The Netherlands.

Kapitza, P.L., 1948, 1949. "Wellenstromung der dunnen schichten einer viskosen flussigkeit". *J Exp Theoret Phys (UdSSR*, p. 18(1):3–18; 19(2):105–120.

Modelica Association, 2007. "Modelica specification". Modelica. 24 june 2020 <http://www.modelica.org/documents>.

Narváez-Romo, B. and Simões-Moreira, J.R., 2017. "Falling liquid film evaporation in subcooled and saturated water over horizontal heated tubes". *Heat Transfer Engineering*, Vol. 38:3, pp. 361 – 376. doi: https://doi.org/10.1080/01457632.2016.1189275.

Nusselt, W., 1916. *Die Oberflachenkondensation des Wasserdampfes*. Z. Vereinsdeutscher Ininuere, 60th edition.

Stephan, P., Kabelac, S., Kind, M., Martin, H., Mewes, D. and Schaber, K., 2010. *VDI Heat Atlas*. Springer-Verlag Berlin Heidelberg, 2nd edition. doi:https://doi.org/10.1007/978-3-540-77877-6.

Teleken, J.G., 2013. *Modelagem matemática e análise fluidodinâmica do processo de destilação por filme líquido descendente*. Ph.D. thesis, Universidade Federal de Santa Catarina, Florianopolis, Brasil.

Ticona, E.M., 2003. *Determinação experimental do coeficiente de troca de calor em um gerador de "pasta de gelo"*. Master's thesis, Pontificia Universidade Catolica do Rio de Janeiro, Rio de Janeiro, Brasil.

Wilke, W., 1962. "Wärmeübergang an rieselfilme". *VDI-Forschungsheft*, Vol. 490.

Zhang, J.T., Wang, B.X. and Peng, X.F., 2000. "Falling liquid film thickness measurement by an optical-electronic method". *Review of Scientific Instruments*, Vol. 71, pp. 1883 – 1886. doi:https://doi.org/10.1063/1.1150557.

## 9. RESPONSIBILITY NOTICE

The authors are solely responsible for the printed material included in this paper.